International Journal Of
Industrial Electronics Control and Optimization
Print ISSN: 3517-2645
Online ISSN: 3568-2645
Homepage: https://ieco.usb.ac.ir/

An Improved Linear Switched Reluctance Motor for Elevator Application

Allahverdi Azadrou1 | Siamak Masoudi2 | Shahla Gharaati3

Department of Electrical Engineering, Islamic Azad University, Salmas Branch, Salmas, Iran. [1]
Department of Electrical Engineering, Islamic Azad University, Abhar Branch, Abhar, Iran. [2]
Administration of education, Salmas, Iran. [3]
Corresponding author's email: Masoudi.elec@gmail.com

Article Info

Article type:
Research Article
Article history:
Received: 05 July 2022
Received in revised form: 04 Oct 2022
Accepted: 15 Oct 2022
Published online: 21 Nov 2022
Keywords:
Linear motor,
Motor Design,
Switched reluctance motor

ABSTRACT

This work deals with minimizing fluctuations of propulsion force and improving the motion quality in a linear switched reluctance motor. In order to minimize the jerks in the moving part of the motor, a new profile is used to generate an appropriate reference speed profile. Then, a simple fuzzy logic system which is able to overcome the uncertainties problem in nonlinear systems is designed and applied to the motor. The fuzzy control system can regulate the motor performance so that it tracks the reference speed with minimum error and fluctuation. The system is designed and its efficiency is shown through simulation and experimental tests in different performance situations. The obtained results confirm that the proposed strategy outperforms other conventional methods.

I. Introduction

Linear electrical motors are efficient and useful instruments in industrial applications with direct motion. Using these motors, rotary to linear motion mechanical converters are eliminated resulting in a simpler, cheaper, and more robust system. Linear switched reluctance motors (LSRMs) have several advantages that distinguish them from other types of electrical motors [1]. LSRMs have only one set of coils on the stator or translator, while the other side has no winding or PM. This feature is especially important in applications that involve a long movement path such as electric trains and elevators in tall buildings. Different LSRMs have been presented which can be used in various applications [1] and [2]. The standard design of LSRMs is done based on the design of corresponding rotary motors [1]. Review of different topologies of linear switched reluctance motor has been done in [3]. Reference [4] reviewed different topologies of LSRMs suitable for vertical motion applications, and finally a structure was selected which has been used in later studies [5] – [9]. The structure selected in the mentioned articles is a good choice for elevator application, though it needs massive iron to be placed for the entire movement path in tall buildings. In [10], a linear switched reluctance motor with additional permanent magnets has been examined in a railway system. The motor tempuratur studies has been done in [11]. The presented motor can create high force dencity, but PMs increase the total cost significantly. Use of more teeth at poles has a good effect on LSRM performance and the propulsion force quality. Two of these structures have been presented in [12] and [13]. The LSRM studied in [13] consisted of a modular toothed linear hybrid reluctance motor with permanent magnets in tranbslator slots. Details of the motor has been explained in [14]. All mentioned single-sided topologies in [10] – [14] were efficient in horizontal movement, but they were not good candidates in vertical motion applications such as elevator systems. Iron loss analysis and flux characteristics of a LSRM have been discussed in [15] and [16]. End-effects of a LSRM were explored in [17] based on mathematical and finite element analysis. A double-sided segmental stator LSRM with a high

Copyright © 2022 Allahverdi et al. Published by University of Sistan and Baluchestan. This work is licensed under a Creative Commons Attribution-Noncommercial 4.0 International license. (https://creativecommons.org/licenses/by-nc/4.0/). Non-commercial uses of the work are permitted, provided the original work is properly cited
DOI: 10.22111/IECO.2022.42777.1437

force density was presented in [18] which can be an appropriate choice for railway applications. A modular-stator LSRM with an active translator was presented in [19], which would produce a good average force though requiring extensive iron to be placed along the entire path in elevator application. In [20], a double-sided yokeless multi-tooth LSRM was proposed consisting of PMs in translator poles. It show a very good performance in terms of force ripple and cogging force. Analysis, design, and optimization of toroidally wound mover LSRM with segmental stator were done in [21] and [22]. A double-sided linear switched reluctance motor with two translators in a common stator was used in elevator application in [23] where the presented system indicated high average force with low ripple. In [24], seeker optimization algorithm was employed to achieve the least force ripple with maximum average force. Influence of design parameters and dimensions in the optimization of LSRM under thermal and weight constraints was discussed in [25]. In order to have a price electromagnetic model of a switched reluctance motor, it is very useful to analyze the flux, inductance, and force characteristics. These were done for two different LSRMs in [26] and [27]. In [28], the magnetic equivalent circuit of the LSRM was utilized to examine the performance of LSRM under asymmetric air-gap. This work presents the design and optimization of a double-sided linear switched reluctance motor with segmented stator and yokeless translator. In order to widen the positive force region, non-uniform air-gap has been designed and optimized. The proposed LSRM offers the advantages of the high force to mass ratio and low total cost. The influence of non-uniform air-gap dimension on the inductance and force characteristics of the motor is investigated and optimized via non-dominated sorting genetic algorithm to offer the maximum average force with minimum ripple. Finite element analysis of the proposed system has been done, and the results have been compared with a conventional LSRM.

II. Selected Structure Of LSRM

A. Elevator application

Fig. 1 displays the schematic view of the proposed LSRM. The motor has a twin opposing segmented stator with a yokeless translator as a motion guide in the path. The stator has eight concentric windings wound around the yoke of phases that are separated mechanically together. The LSRM shown in Fig. 1 has some advantages making it a good candidate for elevator application. In this motor, two phases are fed simultaneously, thus a high-power density is produced. The stator is made segmental and there is almost no mutual inductance between the phases. Hence, in addition to reducing the weight of the moving part, the losses are also reduced. Further, the translator has no yoke, which is very important economically in tall buildings and occupies less space.

B. The main idea

In the elevator application, the force produced by phases is always upward. In ascending motion, this force acts as a propulsion power while in descending motion it prevents the moving part from falling. According to (1), the phase force has a direct relationship with derivative of the inductance. In a conventional structure, a phase inductance is symmetrical in a pole pitch. In an elevator, the phase force generated in the inductance increasing zone ($dL/dx > 0$) is used for both ascent and descent. In this work, by changing the pole shape and the air-gap, the inductance curve becomes asymmetric whereby the inductance ascent side is greater than the other side's. This has two major advantages:

- Positive force is generated in a wider area, so the average force increases.
- Air-gap changes continuously, which is effective in the force ripple reduction.

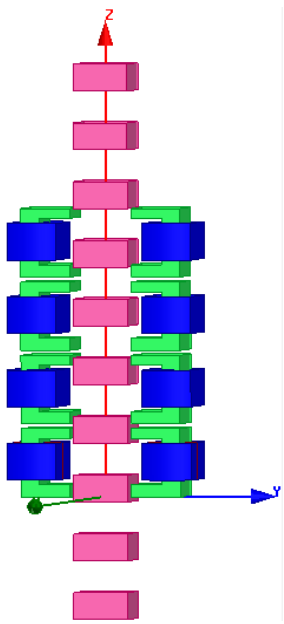


Fig. 1. 3-D FEA model of the proposed LSRM.

The proposed structure and the phase inductance curve are shown in Fig. 2. In a conventional structure, the phase inductance grows and then remains constant in its maximum value, while in the proposed structure, the inductance has a small constant zone with a large positive slope region.

C. Propulsion Force Generation

In the LSRM, the generated phase force in Z-axis direction can be written as [21]:

$$f_z = \frac{1}{2} i^2 \frac{dL}{dz} \quad (1)$$

where, L is the phase inductance and i represents the phase winding current. The average force from unaligned position z_2 to aligned position z_1 is written as:

$$f_{av} = \frac{\int_{z_1}^{z_2} f_z dz}{z_2 - z_1} = \frac{W'_{z=z_1} - W'_{z=z_2}}{dz} = \frac{W'_t}{z_2 - z_1} \quad (2)$$

where, W'_z and W'_t denote the co-energy at position z

and total co-energy from aligned to unaligned position, respectively. Neglecting the energy in the core, we can write the co-energy at the aligned position as:

$$W'_{z_1} = \oint_V \frac{B_g^2}{2\mu_0} dV = \oint_V \frac{(\mu_0 H_g)^2}{2\mu_0} dV =$$
$$\int_0^L \int_0^g \int_0^{w_{sp}} B_g^2(x,y,z)dxdydz = \frac{\mu_0 H_g^2}{2} g L w_{sp}.2\beta_s\gamma \quad (3)$$

where, β_s denotes the ratio of stator pole width to stator pitch, while γ indicates the ratio of translator pole width to stator pole width. In this work, d is assumed to be equal or larger than the stator pole width. This causes the overlap of the poles at aligned position to be approximately same as the conventional structure. Thus, the magnetic resistance at the aligned position will remain almost unchanged.

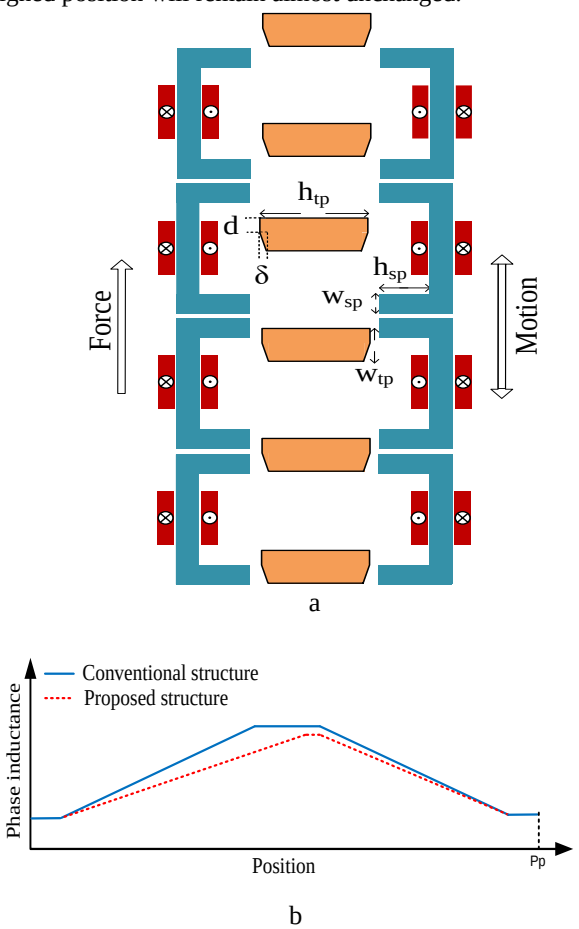


Fig. 2. (a) 2-D model of the proposed LSRM with non-uniform air-gap, (b) Ideal inductance curves.

D. Propulsion Structural Reforms

In order to improve the structure of the LSRM for elevator application, translator poles in Fig. 3-a were changed to a new shape as Fig. 3-b. The results indicated that this change is effective in enhancing the average force and reducing the ripple of force. A new problem is that, in the new structure there is a negative force agree with the earth's gravity in the unaligned position which is due to the asymmetry of the rotor poles. To solve this problem, a pole-shoe was added to the up side of the stator poles as Fig. 3-c. Inductance and force profiles for a phase are depicted in Fig. 4 for three structures. These profiles have been curved based on finite element analysis and the optimized dimensions.

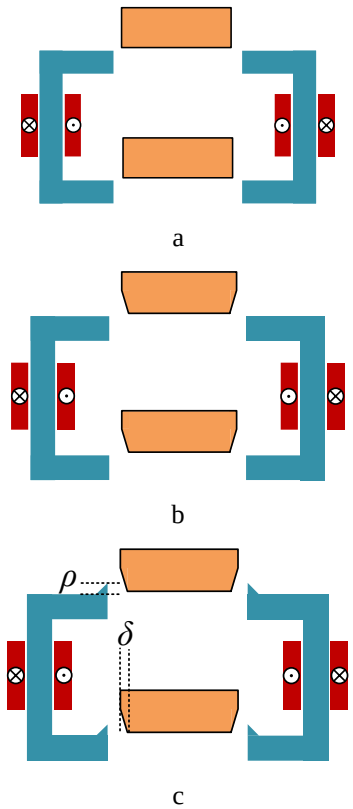


Fig. 3. (a) initial structure- Type 1, (b) translator pole change- Type 2, (c) proposed structure- Type 3.

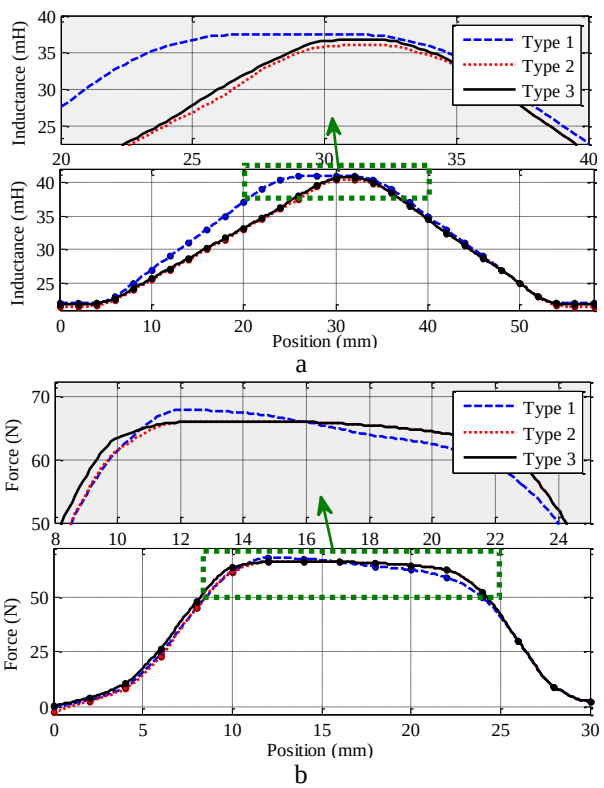


Fig. 4. (a) Inductance profile, (b) Phase force profile.

III. Optimization Of The Structure

A. Multi-Objective Optimization Problem

Multi-objective optimization problem (MOOP) deals with a *K*-dimensional decision space of objective function $\underline{U}(\underline{X}) = \{U_1(\underline{X}), U_2(\underline{X}), \dots, U_q(\underline{X})\}$ based on decision vectors $\underline{X}$. This method includes a set of non-dominated solutions instead of a single optimal method. Minimization of the objective functions leads to a minimum MOOP.

$$Minimize\ \ \underline{U}(\underline{X}) = \{U_1(\underline{X}), U_2(\underline{X}), \dots, U_q(\underline{X})\} \qquad (4)$$

where $\underline{X} = [\underline{X}_1, \underline{X}_2, \dots, \underline{X}_K] \in R^K$ denotes a state in the *K*-dimensional decision space (R^k), and $\underline{U} = [U_1, U_2, \dots, U_q] \in \Omega^q$ is the objective space with q minimization objectives. In this work, the average force, propulsion force ripple, and total mass of the motor have been selected as objective functions [24].

B. Objective Functions

Determining an appropriate objective function is the first step in an optimization problem. Linear switched reluctance motors have inherently high force ripple which limits their applications in various industries. Initially, dimensions of the LSRM should be optimized so that it generates a high average force (F_{av}) with minimal ripple (*RF*) which is defined as ratio of the ripple to the average force in percent. Also, the total mass of the motor (*M*) is another important factor. Accordingly, three objective functions can be determined as follows:

$$u_1(\underline{x}) = \frac{1}{F_{av}} \qquad (5)$$

$$u_2(\underline{x}) = RF \qquad (6)$$

$$u_3(\underline{x}) = M \qquad (7)$$

where, *x* denotes a vector including all dimension variables that may be adjusted to optimize the objective functions. Given some structural limitations, the parameters denoted in Fig. 2-a have been considered as optimization dimensions. The air-gap is considered constant 2 mm in the work. Hence, the adjustable parameters vector can be written as:

$$\underline{x} = (w_{sp}, w_{tp}, h_{sp}, h_{tp}, \delta, d, \rho) \qquad (8)$$

C. Multi-Objective Optimization

Dimensions of the LSRM denoted as x vector are changed and functions (5) – (7) are calculated at each step. The process continues until the function (9) reaches its minimum value.

$$f = min\ \{u_1, u_2, u_3\} \qquad (9)$$

In this work, the non-dominated sorting genetic algorithm (NSGA II) presented in [29] has been employed to solve the optimization problem. In this algorithm, the objective functions are calculated and the initial populations are sorted based on non-domination into each front. In the second step, crossover and mutation are performed. Identification of non-dominated individuals from the first front population occurs in the third step which is the ranking step. The non-dominated set of solutions creates the first front solution whose individuals dominate the second front individuals. Thus, the front continues and all the fronts are determined. In each font, the sort values are described by individuals with specified crowding distance. By knowing the sort values and crowding distance, all of the first solutions or individuals are selected based on competition selection. The offspring population is developed from crossover and mutation operators. The best K individuals are chosen and the populations including the current population and offspring populations are ranked based on non-domination. The process continues until the stopping conditions are met. In the proposed optimization algorithm, population size, crossover probability, mutation probability, and maximum gen are 25.4, 0.8, 0.01, and 100 respectively, while the process has 100 independent runs.

IV. Simulation Results

The LSRM displaced in Fig. 3 – c was optimized through the genetic algorithm mentioned in the previous section. Some parameters which are constant are reported in TABLE 1.

TABLE 1
CONSTANT PARAMETERS OF THE LSRM

Parameter	value
air-gap length	2 mm
turns in each coil	240 turns
rated voltage	150 v
rated current	12 A
friction coefficient	25 N/m/s
phase resistance	2.8 **Ω**

For better and more accurate conclusions, both Type 1 and Type 3 LSRMs were optimized whereby the values indicated in TABLE 2 were obtained.

TABLE 2
OPTIMIZED PARAMETERS OF THE LSRM

Parameter	Initial	Optimized Type 1	Optimized Type 3
w_{sp}	14 mm	15 mm	15.5 mm
w_{tp}	28 mm	34 mm	33 mm
h_{sp}	30 mm	32 mm	31 mm
h_{tp}	36 mm	34 mm	30 mm
d	14 mm	---	15 mm

δ	4 mm	---	3 mm
ρ	3 mm	---	3.5 mm

Finite element analysis of three types LSRMs was performed through Maxwell 16. In the analysis, the stator is moved by 1-mm steps along a pole pitch, where the phase force as well as inductance is recorded at each point. The data obtained have been plotted in Fig. 4 using the curve fitting algorithm. The results in three aligned, mid-aligned, and un-aligned positions for three structures are presented in Fig. 5.

Fig. 6 compares the average force and the ripple of the propulsion force at nominal current. It can be observed that the proposed structure has a higher average value. In order to achieve a complete comparison, the average force and the ripple for different phase currents are indicated in TABLE III. In the table, Fav denotes the average force and RF indicates the ration ripple to the average force in percent. It can be seen that the proposed structure has fewer force ripples due to the gradual reduction of the air-gap length. Further, the average force in the proposed structure is higher which is due to the wider phase force.

TABLE 3
OPTIMIZED PARAMETERS OF THE LSRM

Phase current		**3 A**	**6 A**	**9 A**	**12 A**
Type 1	$F_{av}(N)$	22	48	94	152
	RF (%)	5.2	6.5	7.1	7.2
Type 2	$F_{av}(N)$	28	53	99	159
	RF (%)	4.6	5.8	6.3	6.3
Type 3	$F_{av}(N)$	31	56	104	163
	RF (%)	3.4	3.6	4.1	4.1

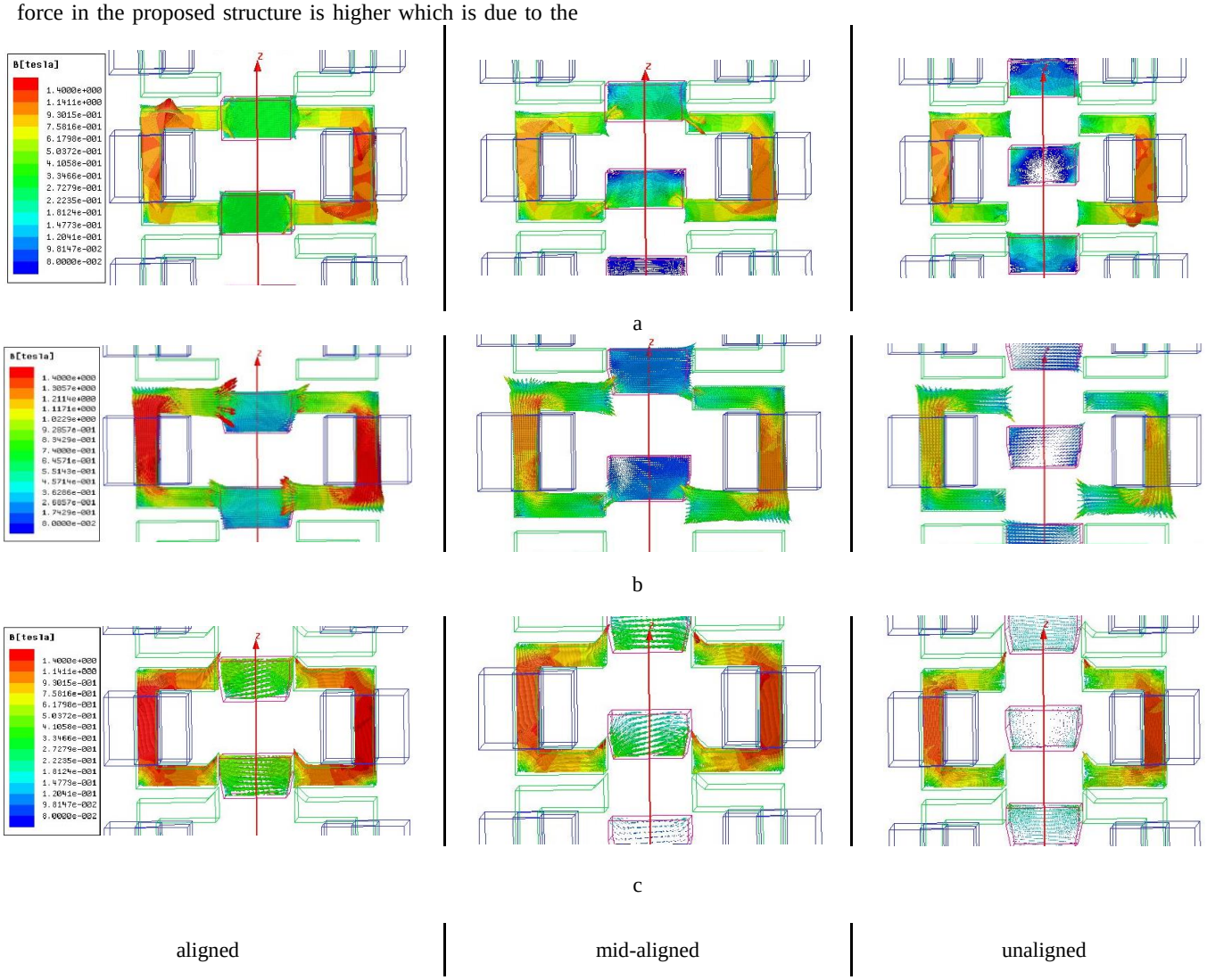


Fig. 5. Finite element analysis of three structures, (a) Type 1, (b) Type 2, (c) Type 3

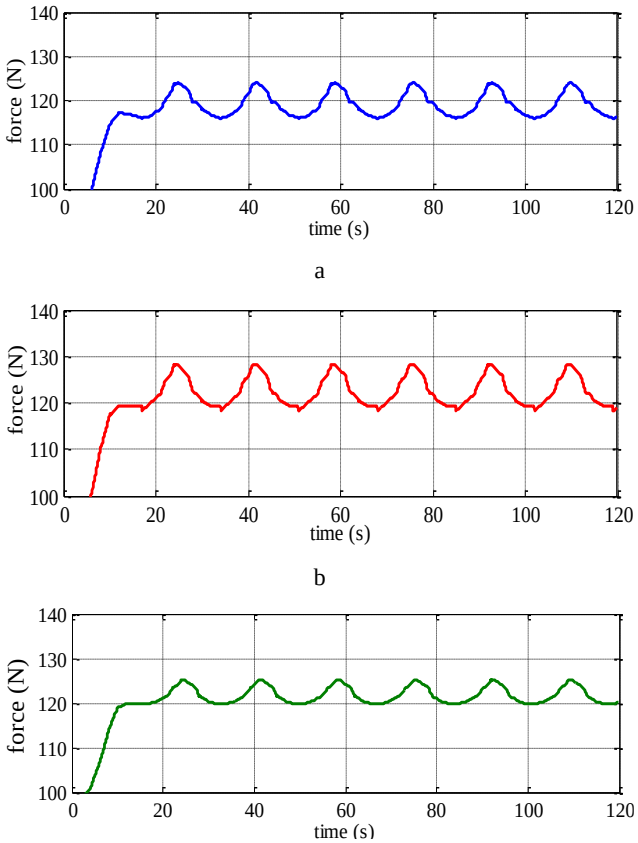


Fig. 6. Propulsion force at i=10 A, (a) Type 1, (b) Type 2, (c) Type 3.

V. Experimental results

To demonstrate the performance of the proposed structure, both type 1 and type 3 structures with the dimensions expressed in Tables I and II were constructed and compared experimentally. Both the stator and translator cores are made of silicon steel sheets. All poles need careful installation because of the poles of the stator and translator are separated individually due to no back iron. Thus, poles of both stator and translator are mounted on aluminum frames with a fixed distance of 2 mm as the initial air gap. A spacer is installed to ensure the constant distance. The structures of the LSRM are shown in Fig. 7. Propulsion force and inductance of the LSRMs are measured after locking the moving part using a plate and connectors at the desired position and energizing one phase winding with a constant DC current through a PWM power converter. A load cell sensor has been used to record the propulsion force data at a steady state current. For the inductance measurement, the angle between input voltage and current is determined from an oscilloscope. Results obtained from the mentioned experimental tests (EXP) are shown in Fig. 80 compared with the finite element analysis (FEA). Results indicate that the practical results are relatively close to the finite element analysis results. This confirms the performance of the proposed structure of the LSRM for the elevator application as a unidirectional motion industry.

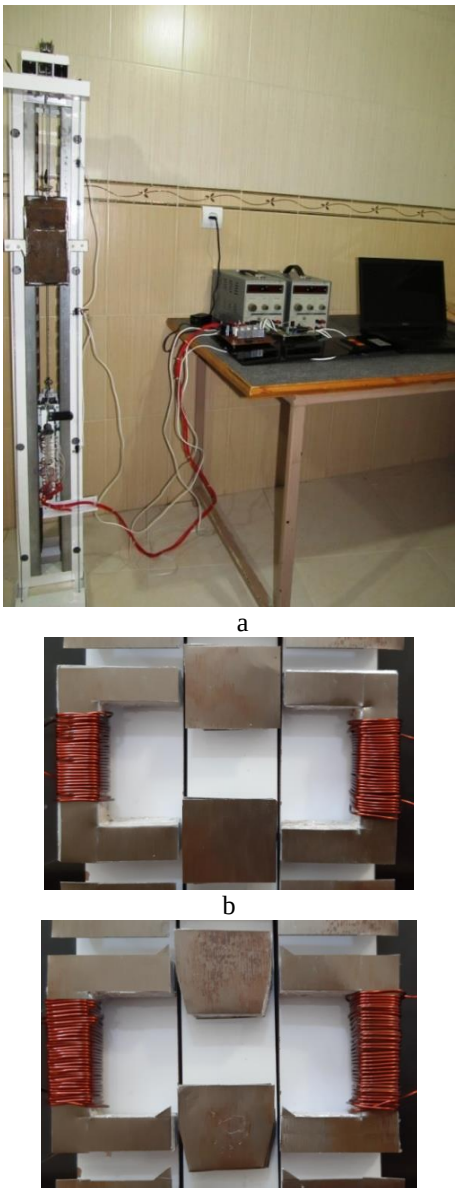


Fig. 7.(a) Prototype system, (b) Poles for Type 1, (c) Poles for Type 3.

VI. Conclusions

This work demonstrated the design and optimization of a linear switched reluctance motor for the elevator application. The propulsion force in the proposed structure was always upward corresponding to the working characteristics of an elevator. The translator was without yoke, making the system light and suitable economically, while the stator included separate poles leading to minor core losses. The translator was designed with a non-uniform air-gap length to generate wider positive force region and thus higher average force. Finite element analysis of the proposed structure along with a conventional one was performed and compared. A prototype system with two type 1 and type 3 pole structures was constructed and practical tests were performed. The obtained results were very close to the finite element analysis results confirming the robustness of the proposed structure.

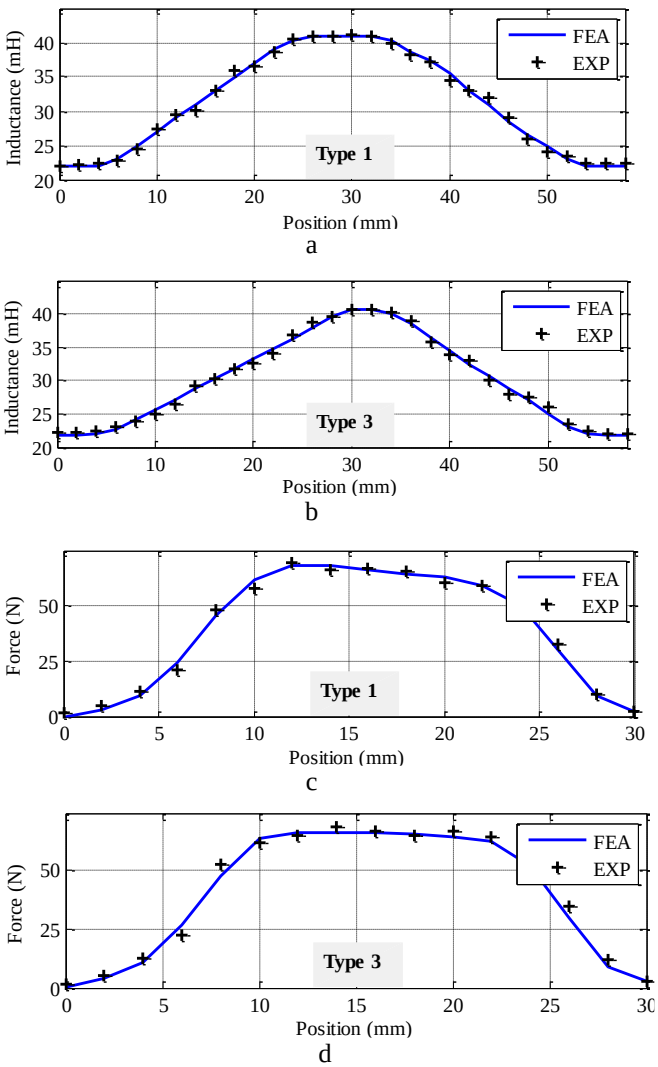


Fig. 8. Comparison of the experimental results and finite element results, (a) Inductance, Type 1, (b) Inductance Type 3, (c) Phase force Type 1, (d) Phase force Type 3.

REFERENCES

[1] Krishnan, R., 'Switched reluctance motor drives: modeling, simulation, analysis, and applications', CRC Press, Boca Raton, 2001.

[2] N. Prasad, S. Jain, S. Gupa, "FEM based analysis and design of linear switched reluctance motor topologies for high speed transit application," 2021 2nd International Conference on Electrical Power and Energy Systems (ICEPES), Bhopal, India, 2021.

[3] N. Prasad, S. Jain, S. Gupa, "Review of linear switched reluctance motor designs for linear propulsion applications", CES Transactions on Electrical Machines and Systems, vol. 6, no. 2, pp. 179-187, 2022.

[4] H. S. Lim, R. Krishnan, "Ropleless elevator with linear switched reluctance motor drive actuation systems", IEEE Trans. Ind. Electron., vol. 54, no. 4, pp. 2209-2217, 2007.

[5] H. S. Lim, R. Krishnan, N. S. Lobo. "Design and control of a linear propulsion system for an elevator using linear switched reluctance motor drives," IEEE Trans. Ind. Electron. vol 55, no. 2, pp. 534-542. Jan 2008.

[6] S. Masoudi, M. R. Feyzi, M. B. B. Sharifian. "Force ripple and jerk minimization in double sided linear switched reluctance motor used in elevator application," IET Elec. Pow. Appl. vol. 10, no. 6, pp. 508-516. Jun 2016.

[7] S. Masoudi, M. R. Soltanpour, H. Abdollahi. "Adaptive fuzzy control method for a linear switched reluctance motor," IET Elec. Pow. Appl. vol. 12, no. 9, pp. 1328-1336, Nov 2018.

[8] A. Azadrou, S. Masoudi, R. Ghanizadeh, P. Alemi. "New adaptive fuzzy sliding mode scheme for speed control of linear switched reluctance motor," IET Elec. Pow. Appl. vol. 13, no. 8, pp. 1141-1149, 2019.

[9] A. Azadrou, S. Masoudi, R. Ghanizadeh, P. Alemi. "Improving Quality of Movement in a Linear Switched Reluctance Motor Using a Fuzzy Logic System," International journal of industrial Electronics, Control and Optimization, vol. 3, no. 4, pp. 459-468, 2020.

[10] R. Cao, E. Su, M. Lu, "Comparative study of permanent magnet assisted linear switched reluctance motor and linear flux switching permanent magnet motor for railway transportation," IEEE Transaction on Applied Superconductivity, vol. 30, no. 4, 2020.

[11] M. Lu, R. Cao, "Comparative investigation of high temperature superconducting linear switched flux-reluctance motor and high temperature superconducting linear switched reluctance motor for urban railway transit," IEEE Transaction on Applied Superconductivity, vol. 31, no. 5, 2021.

[12] H. J. Liang, S. D. Huang, G. Z. Cao, T. Liang, "Design and analysis of a large-thrust and small-deformation double-sided linear switched reluctance motor," 5th International Electrical and Energy Conference (CIEEC), Nangjing, Chaina, 2022.

[13] M .Vatani, A. Ghaffarpour, M. A. J. Kondelaji, M. Mirsalim, "Study of a toothed linear hybrid reluctance motor with permanent magnets in translator slots," IEEE Trans. On Transportation Electrification, vol. 8, no. 3, pp. 3554-3567, 2022.

[14] M. Vatani, M. Mirsalim, "The modular and crooked-tooth translator linear switched reluctance motor with a high-thrust per weight," IEEE Trans. On Transportation Electrification, vol. 7, no. 3, pp. 3554-3567, 2021.

[15] H. Chen, W. Yan, K. Wang, "Iron loss analysis of double-sided linear switched reluctance launcher," IEEE Transactions on Plasma Science, vol. 47, no. 5, pp. 2323-2330, 2019.

[16] H. Chen, W. Yan, K. Wang, "Electromagnetic analysis of flux characteristics of double-sided switched reluctance linear machine," IEEE Transactions on Applied Superconductivity, vol. 26, no. 4, 2016.

[17] Z. Zhang, N. C. Cheung, K. W. E. Cheng, X. D. Xue, J. K. Lin, "Longitudinal and transversal end-effect analysis of linear switched reluctance motor," IEEE Transaction on Magnetics, vol. 47, no. 10, pp. 3979-3983, 2011.

[18] D. Wang, X. Wang, X. F. Du, "Design and comparison of a high force density dual side linear switched reluctance motor for long rail propulsion application with low cost," IEEE Transaction on Magnetics, vol. 53, no. 6, 2017.

[19] M. Vatani, M. Mirsalim, "Comprehensive research on a modular-stator linear switched reluctance motor with a toroidally wound mover for elevator applications," 10th

International Power Electronics, Drive Systems and Technologies Conference (PEDSTC), Shiraz, Iran, Feb. 2019.
[20] Y. Shen, Q. Lu, H. Li, J. Cai, X. Huang, Y. Fang, "Analysis of a novel double-sided yokeless multi-tooth linear switched-flux PM motor," IEEE Trans. On Ind. Elec., vol. 65, no. 2, pp. 1837-1845, 2018.
[21] D. Wang, X. Du, D. Zhang, X. Wang, "Design, optimization, and prototyping of segmental-type linear switched – reluctance motor with a toroidally wound mover for vertical propulsion application," IEEE Trans. On Ind. Elec., vol. 65, no. 2, pp. 1865-1874, 2018.
[22] J. F. Pan, L. Qui, J. Zhu, B. Zhang, "Optimal positioning coordination for multiple linear switched reluctance machines," IEEE Transaction on Magnetics, vol. 53, no. 11, 2009.
[23] S. Masoudi, H. Mehrjerdi, A. Ghorbani, "New elevator system constructed by multi-translator linear switched reluctance motor with enhanced motion quality," IET Electric Power Application, vol. 14, no. 9, pp. 1692-1701, 2020.
[24] M. R. Soltanpour, H. Abdollahi, S. Masoudi, "Optimisation of double-sided linear switched reluctance motor for mass and force ripple minimisation," IET Science, measurement and technology, vol. 13, no. 4, pp. 509-517, 2019.
[25] J. G. Amoros, P. Andrada, B. Blangue, M. M. Genesca, "Influence of design parameters in the optimization of linear switched reluctance motor under thermal constraints," IEEE Transaction on Ind. Elec., vol. 65, no. 2, pp. 1875-1883, 2018.
[26] H. Chen, X. Liu, W. Yan, "Three-dimentional magnetic equivalent circuit research of double-sided switched reluctance linear machine," IEEE Trans. On Applied Superconductivity, vol. 30, no. 4, 2020.
[27] W. Zaafrane, M. Dursun, "Double sided linear switched reluctance motor analysis and modeling including end-effect," 5th International Conference on Electrical and Electronic Engineering (ICEEE), Istanbul, Turkey, 2018.
[28] H. Chen, W. Yan, "Flux characteristics analysis of double-sided switched reluctance linear machine under asymmetric air gap," IEEE Trans. On Ind. Elec., vol. 65, no. 12, pp. 9843-9852, 2018.
[29] K. Deb, A. Pratap, S. Agarwal, "A fast and elitist multi-objective genetic algorithm: NSGA-II," IEEE Trans. on Evolutionary Computation, vo;. 6, no. 2, pp. 182-197, 2002.
[30] K. S. Ha; S. G. Oh, B. MacCleery, and R. Krishnan, "An automated reconfigurable FPGA-based magnetic characterization of switched reluctance machines," in Proc. of the IEEE International Symposium on Industrial Electronics, vol. 2, pp. 839 – 844, 2005.



Allahverdi Azadrou was born in Salmas, Iran, in 1983. He received his B.S. degree in electrical engineering from Islamic Azad University, Abhar Branch, Abhar, Iran, and M.S. degree from Dezful Branch, Dezful, Iran. He is a member of science in Islamic Azad University, Salmas Branch, Iran since 2012. Currently he is Ph.D student in Islamic Azad University, Urmia Branch, Urmia, Iran.



Siamak Masoudi was born in Miyaneh, Iran. He received his B.S. degree in power engineering from Tarbiat Moallem Tabriz University, Tabriz, Iran, in 2006, and his M.S. and Ph.D. degrees in Electrical Machines and Drives from University of Tabriz, Tabriz, Iran, in 2009 and 2016, respectively. From 2010, he is a member of science in Islamic Azad University, Abhar Branch, Zanjan, Iran. His current research interests include Electrical machines design and control and linear motors/generators.



Shahla Gharaati was born in Salmas, Iran, in 1986. He received his B.S. and M.S. degrees in electrical engineering Islamic Azad University, Urmia Branch, Urmia, Iran in 2009, and 2013, respectively. She works in administration of education in Salams, Iran.